AN INTEGRATED APPROACH FOR ORTHOIMAGE AND DTM GENERATION USING MARS EXPRESS HRSC DATA

S. Gehrke, I. Haase

Technische Universität Berlin, Geodesy and Geoinformation Science, Berlin, Germany –
stephan@igg.tu-berlin.de, isabel.haase@gmx.de

Commission IV, WG IV/7

KEY WORDS: Planetary, Photogrammetry, Three-Line, Matching, Orthoimage, DEM/DTM

ABSTRACT:

The *High Resolution Stereo Camera* (HRSC) on *Mars Express* covers the surface of our neighboring planet in full color and 3D. Altogether, nine channels are obtained in stereo angles between ±18.9°. These data sets are well suited to derive Digital Terrain Models (DTM) and, based on that, color orthoimages. Both, photogrammetric standard processing of HRSC data as well as alternative and/or supplementary approaches are usually based on image matching or shape-from-shading.
In contrast to classical matching between images – and aiming for the combined derivation of orthoimage, DTM, and reflectance properties of the Martian surface – HRSC data are processed using the *Facets Stereo Vision* approach, which is a flexible method for matching in object space. Transfer functions connect the object surface (surfels) with corresponding pixels in each image; the entire image content is treated as observables. The unknowns, in particular an orthoimage (brightness values) and a DTM (height values), are estimated in a combined least squares adjustment with respect to spatially regular grids in object space, i.e. the facets. Thus, existing interconnections between these models are implicitly regarded. In this context, an indirect approach of *Facets Stereo Vision* is utilized for the processing of HRSC data. It is implemented with MATLAB and applied for small Martian regions with varying surface characteristics. Exemplarily, the results for a steep crater rim and a comparatively flat region are presented and judged.

KURZFASSUNG:

Die *High Resolution Stereo Camera* (HRSC) auf *Mars Express* bildet die Oberfläche unseres Nachbarplaneten in Farbe und 3D ab. Insgesamt werden neun Kanäle in Stereowinkeln zwischen ±18.9° simultan aufgenommen. Diese Daten sind prädestiniert für die Ableitung von Digitalen Geländemodellen (DGM) und, darauf aufbauend, von Orthobildern. Sowohl die photogrammetrische Standardprozessierung als auch alternative bzw. ergänzende Ansätze zur Auswertung von HRSC-Daten basieren auf Bildzuordnung (Image Matching) bzw. auf Shape-from-Shading.
Im Gegensatz zum klassischen Matching zwischen Bildern – und mit dem Ziel der gemeinsamen Ableitung von Orthobild, DGM und Reflexionseigenschaften der Mars-Oberfläche – werden in diesem Rahmen HRSC-Daten mit dem *Facetten-Stereosehen* ausgewertet, einem flexiblen Algorithmus der Bildzuordnung im Objektraum. Transferfunktionen verbinden dabei die Objektoberfläche (Surfel) mit den korrespondierenden Pixeln in jedem Bild; sämtliche Pixel und daher die gesamten Bildinformationen werden als Beobachtungen behandelt. Die Unbekannten, grundsätzlich das Orthobild (Helligkeitswerte) und das DGM (Höhenwerte), werden in einer Ausgleichung nach der Methode der kleinsten Quadrate bezüglich regelmäßiger Lageraster, den Facetten, geschätzt. Damit sind die zwischen diesen Objektmodellen existierenden Zusammenhänge implizit berücksichtigt. Für die Auswertung von HRSC-Daten wird hier mit dem indirekten Ansatz des *Facetten-Stereosehens* gearbeitet. Er ist in MATLAB implementiert und auf Bilddaten verschiedener, kleiner Regionen der Mars-Oberfläche angewendet. Erste Ergebnisse dieser Untersuchungen werden am Beispiel eines Einschlagkraters sowie eines vergleichsweise flachen Talverlaufs präsentiert und bewertet.

1. INTRODUCTION

Since 2004, the *High Resolution Stereo Camera* (HRSC) experiment on board of the *Mars Express* mission systematically covers the surface of our neighboring planet providing both color and stereo. Nine channels are obtained simultaneously, in particular four color channels (red, green, blue, and infrared) as well as five panchromatic channels, arranged in stereo angles between 0° (nadir), ±12.9° (photometry), and ±18.9° (stereo). The maximum ground resolution is 12 m/pixel in nadir. Stereo and photometry channels are usually stored in macropixel formats: 2x2 or 4x4 pixels, respectively, are combined (*Neukum* et al., 2004). HRSC data are well suited to derive Digital Terrain Models (DTM) and, based on that, color orthoimages. Within a few days after its acquirement, each HRSC orbit is processed automatically at *German Aerospace Center* (DLR). Depending on ground resolution, the resulting orthoimages feature up to 12.5 m/pixel. Automatically generated DTM data are commonly sampled with respect to a 200 m grid (*Scholten* et al., 2005). Besides, alternative and/or supplementary approaches are investtigated within the *HRSC Co-Investigator Team*, such as the adaptation of HRSC orbits to MOLA (see chapter 2.3). Based on such improvements and making use of adaptive processing components, high quality HRSC DTMs can be derived (*Gwin-*

ner et al., 2005). An overview of various approaches is given by *Albertz* et al. (2005); for comparison of results see *Heipke* et al. (2006). Both systematic photogrammetric processing and improvements are either based upon classical image matching or shape from shading, respectively.
In contrast to that, HRSC data are exemplarily processed by matching in object space, i.e. using the *Facets Stereo Vision* approach (*Wrobel*, 1987; *Weisensee*, 1992; *Schlüter*, 2000). This algorithm allows for the integrated computation of orthoimage, DTM, and reflectance model of the Martian surface and, therefore, implicitly considers the existing interconnections. First experiences for the application to the Martian surface have been gained by *Anderssohn* (2004), who used simulated images derived from HRSC orthoimages and DTM data, and *Gehrke* et al. (2006). The *Facets Stereo Vision* approach has been adapted to *Mars Express*' orbit and imaging conditions and to HRSC line-scanner geometry. It is implemented with MATLAB and exemplarily applied for different regions of Mars.

2. MATCHING IN OBJECT SPACE: FACETS STEREO VISION

Facets Stereo Vision is a powerful and flexible algorithm for matching in object space. It was invented by *Wrobel* (1987) and further developed, e.g., by *Weisensee* (1992), *Wrobel et al.* (1992), and *Wendt* (2002). An approach for processing airborne line-scanner imagery based on this algorithm – which could be adapted to HRSC on *Mars Express* in a similar manner – has been proposed by *Schlüter* (2000).

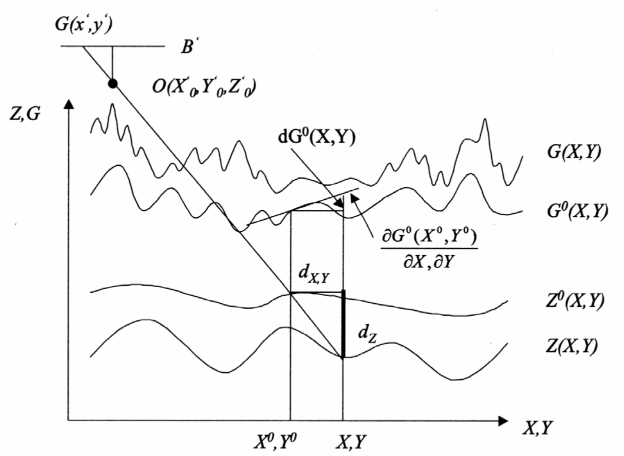

Fig. 1: *Facets Stereo Vision* – relation between object heights Z and grey values G (initial values Z^0 and G^0) and the image G'(x',y') (*Wendt*, 2002).

In general, object surface elements (surfels) are linked with the corresponding pixels in each image with radiometric transfer functions and, geometrically, through the well-known collinearity equations. Compared to classical image correlation, which comprises the matching of certain points or features, all pixels and therefore the entire image contents are treated as observables. The unknowns consist of the orthoimage (brightness values) and the DTM (height values). Both of these object properties are estimated in a combined least squares adjustment with respect to spatially regular grids, i.e. the facets. The existing interconnections are regarded by employing appropriate interpolation functions, which could be bilinear for most cases (*Weisensee*, 1992).

2.1 Basic Equations

The object surface (surfels) and all images (pixels) are interconnected geometrically by camera position and attitude and radiometrically by reflectance properties (Fig. 1). Radiometric relations between the object grey values G(X,Y) and the images G'(x',y'), G''(x'',y''), etc. are modeled with transfer functions T', T'', etc. for every image:

$$G\left(X,Y\right)=T'\left[G'\left(x',y'\right)\right]=T''\left[G''\left(x'',y''\right)\right]=\ldots \tag{1}$$

Expanding G(X,Y) into a *Taylor* series around (X^0,Y^0) gives

$$\begin{aligned}G\left(X,Y\right)&=G^0\left(X^0+dX,Y^0+dY\right)+dG^0\left(X^0,Y^0\right)\\&\approx G^0\left(X^0,Y^0\right)+\frac{\partial G^0\left(X^0,Y^0\right)}{\partial X}dX\\&\quad+\frac{\partial G^0\left(X^0,Y^0\right)}{\partial Y}dY+dG^0\left(X^0,Y^0\right)\end{aligned}\quad , \tag{2}$$

where the lateral displacements dX and dY are connected with height changes dZ through an image ray between the camera at (X'_0,Y'_0,Z'_0) and an object point (X^0,Y^0,Z^0) – cf. Fig. 1:

$$dX=\frac{\partial X}{\partial Z}dZ=\frac{X^0-X'_0}{Z^0-Z'_0}dZ=X'_Z\,dZ \tag{3}$$

$$dY=\frac{\partial Y}{\partial Z}dZ=\frac{Y^0-Y'_0}{Z^0-Z'_0}dZ=Y'_Z\,dZ \tag{4}$$

With (3) and (4) the combination of (1) and (2) leads to the basic equation of *Facets Stereo Vision*. It relates image grey values on the left side with object grey values, heights, and the reflectance model (transfer function) on the right:

$$G'\left(x',x'\right)=T'^{-1}\left\{\begin{matrix}G^0\left(X^0,Y^0\right)+dG^0\left(X^0,Y^0\right)\\+\left[\begin{matrix}\dfrac{\partial G^0\left(X^0,Y^0\right)}{\partial X}X'_Z\\+\dfrac{\partial G^0\left(X^0,Y^0\right)}{\partial Y}Y'_Z\end{matrix}\right]dZ\end{matrix}\right\} \tag{5}$$

In order to derive object brightness values and heights, sampling points with respect to regular grids have to be defined in object space (see below). The object properties can then be estimated in a least squares adjustment based on equation (5).

2.2 Object Models

For modeling DTM and orthoimage, spatially regular facets are defined in object space; the sampling points are given through (X_i,Y_j) and (X_k,Y_l), respectively. An arbitrary point within these facets can be described by piecewise polynomial functions, usually carried out as bilinear interpolations. Thus, initial object heights and height changes can be written as follows:

$$Z^0\left(X^0,Y^0\right)=\sum_i\sum_j\alpha_{ij}\left(X^0,Y^0\right)Z^0{}_{ij} \tag{6}$$

$$dZ\left(X^0,Y^0\right)=\sum_i\sum_j\alpha_{ij}\left(X^0,Y^0\right)dZ_{ij} \tag{7}$$

Similarly, the grey value interpolations in the orthoimage are:

$$G^0\left(X^0,Y^0\right)=\sum_k\sum_l \alpha_{kl}\left(X^0,Y^0\right)G^0{}_{kl} \tag{8}$$

$$dG^0\left(X^0,Y^0\right)=\sum_k\sum_l \alpha_{kl}\left(X^0,Y^0\right)dG_{kl} \tag{9}$$

The grey value gradients – as needed in equation (5) – can be expressed with regard to the same grid:

$$\frac{\partial G^0\left(X^0,Y^0\right)}{\partial X}=\sum_k\sum_l \frac{\partial G^0\left(X^0,Y^0\right)}{\partial \alpha_{kl}\left(X^0,Y^0\right)}\frac{\partial \alpha_{kl}\left(X^0,Y^0\right)}{\partial X} \tag{10}$$

$$\frac{\partial G^0\left(X^0,Y^0\right)}{\partial Y}=\sum_k\sum_l \frac{\partial G^0\left(X^0,Y^0\right)}{\partial \alpha_{kl}\left(X^0,Y^0\right)}\frac{\partial \alpha_{kl}\left(X^0,Y^0\right)}{\partial Y} \tag{11}$$

However, the sampling points do not have to be identical for orthoimage and DTM; the latter model is usually sampled with lower resolution.

2.3 Approach for the Processing of HRSC Data

In contrast to *Schlüter* (2000), who carried out the direct method of *Facets Stereo Vision* to process line scanner imagery, we apply the indirect method to process HRSC data. Such an approach has already been suggested by *Weisensee* (1992) and *Diehl & Heipke* (1992). *Anderssohn* (2004), using simulated imagery, and *Gehrke* et al. (2006) have successfully tested it for the Martian surface.

For applying the indirect method, so called pseudo orthoimages (i.e. pseudo observables) have to be resampled for each HRSC channel. In particular, the object surfels (X_k,Y_k) are projected into each image using initial height values Z^0 and the known camera orientation parameters (see below). Then both grey values and camera orientations are interpolated between adjacent image lines – since each HRSC line features its own position, this is an iterative process. As a result, the (pseudo) observables for the indirect approach are now regularly sampled with respect to the orthoimage facets and, therefore, the least squares adjustment simplifies – cp. equations (8) through (11). Following the proposal of *Weisensee* (1992) and *Anderssohn's* (2004) investigations, the derivations of orthoimage and object heights are separated. In particular, the orthoimage results from the mean value of all pseudo orthoimages. As a consequence thereof – since the DTM has considerably less sampling points – the number of unknowns in the adjustment itself then reduces significantly (cp. equation (5)).

Based on the pseudo observables, the orthoimage as well as height corrections with respect to the initial DTM are calculated. Concerning the radiometric model, linear functions are applied in this study in order to adjust contrast and brightness differences between the images. The entire *Facets Stereo Vision* algorithm has to be carried out iteratively, starting with resampling of pseudo orthoimages using the enhanced DTM heights of the previous calculation, until the termination constraint (no significant height changes) is reached.

Within our investigations we make use of the results of the bundle block adjustment, in which the camera orientations are adapted to the *Mars Observer Laser Altimeter* (MOLA) DTM. This DTM provides the best global data set for Mars (*Smith* et al., 2001). As a result, the spacecraft position errors reduce from approximately 1000 m to 30 m after bundle adjustment (*Spiegel* et al., 2005). Therefore, these orientation parameters remain unchanged in our calculations. Furthermore, the calibrated inner orientation of HRSC is regarded to be constant. Sufficient initial height values are provided through the MOLA DTM which features a sample point distance of 5 km.

3. APPLICATION TO HRSC DATA OF MARS

The adapted, indirect algorithm of *Facets Stereo Vision* is implemented with MATLAB and applied to HRSC data. In comparison to systematic processing of entire orbits, only small regions can be investigated.

3.1 Investigation Areas

For carrying out *Facets Stereo Vision* on Mars, two areas featuring different surface characteristics have been chosen within the Xanthe Terra region (Fig. 2):

- **Valley** (313.4° east / 9.2° north; 5.4x5.4 km). This area in Hypanis Valles is partly covered with debris of the close-by impact event. It is comparatively flat, showing overall height variations below 200 m.
- **Crater rim** (313.4° east / 8.9° north; 5.4x5.4 km). The southern rim of this small unnamed impact crater slopes down more than 1000 m.

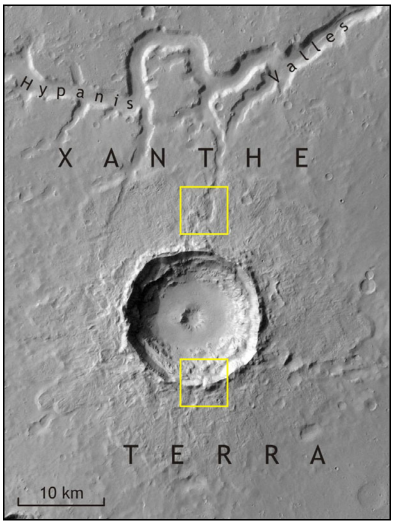

Fig. 2: Investigation areas – valley (north) and crater (south).

3.2 HRSC Input Data

The investigation areas have been covered during *Mars Express* orbit 894. HRSC nadir and two outermost stereo channels, featuring resolutions of 15 m/pixel and 30 m/pixel, respectively, are used as input. Mean (pseudo) orthoimages as well as difference images of the stereo channels are shown in Fig. 3 (left). Considering the areas' sizes of 5.4x5.4 km and the DTM resolution of 5 km, it stands out that no morphologic details are resolved (see Fig. 4, top, and Fig. 5). Such height deviations of the (initial) DTM affect the (initial) pseudo orthoimages; in particular, lateral displacements are caused – cp. equations (3) and (4). This effect is illustrated in the mean images (Fig. 3, left), where, e.g., the elevated crater rim (cp. Fig. 5) can be recognized three times, and also in the difference images of the stereo channels (right). Height deviations in the order of magnitude of a few 100 m are to be corrected by *Facets Stereo Vision*.

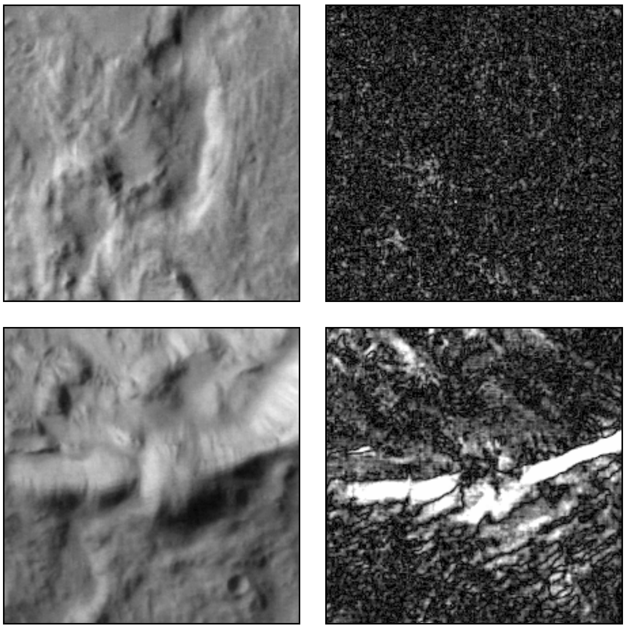

Fig. 3: Mean orthoimages (left) and difference images (right) based on the initial DTM for the valley region (top) and the crater rim (bottom); contrast/brightness enhanced.

3.3 Derivation of Orthoimage and DTM

The combined derivation of orthoimage and DTM presumes the definition of appropriate facets. Taking the nadir and stereo channel resolutions into account, an intermediate value of 25 m has been chosen for the orthoimage. Since the investigation area measures 5400x5400 m, the image sizes are 217x217 pixels. Based on the experiences of *Anderssohn* (2004), *Facets Stereo Vision* is carried out starting with comparatively large DTM facets of 900x900 m, which are then decreased during four subsequent calculation steps to 200x200 m (see Table 1). The resulting heights of each adjustment, after 3x3 low pass filtering (cf. *Gehrke* et al., 2006), provide the initial values for the next step. Finally, the topography of each area is represented by 27x27 facets with the same resolution as the systematically processed HRSC DTM.

DTM facet size in [m]	900^2	450^2	300^2	200^2
Number of DTM facets	6^2	12^2	18^2	27^2
Image pixels per DTM facet	36^2	18^2	12^2	8^2

Table 1: Facet sizes for subsequent data processing.

Each calculation step is carried out in 10 iterations. For all least squares adjustments, the observables consist of all pixels (217^2) in each of three input images, altogether a number of 141,267. The unknown DTM parameters increase from $49 = (6+1)^2$ to $784 = (27+1)^2$. Results for selected iterations, median height corrections and standard deviations, are shown in Table 2.

In Fig. 4, the DTM generation for the valley region is illustrated in perspective views: the initial the MOLA DTM, which only shows a slight overall slope of the terrain, the result of the first calculation step with 900 m facets, where the valley depressions and the two south-western hills are already visible, and the final result based on a sample point distance of 200 m. For the crater rim, a combined view of MOLA and the final DTM is given by Fig. 5.

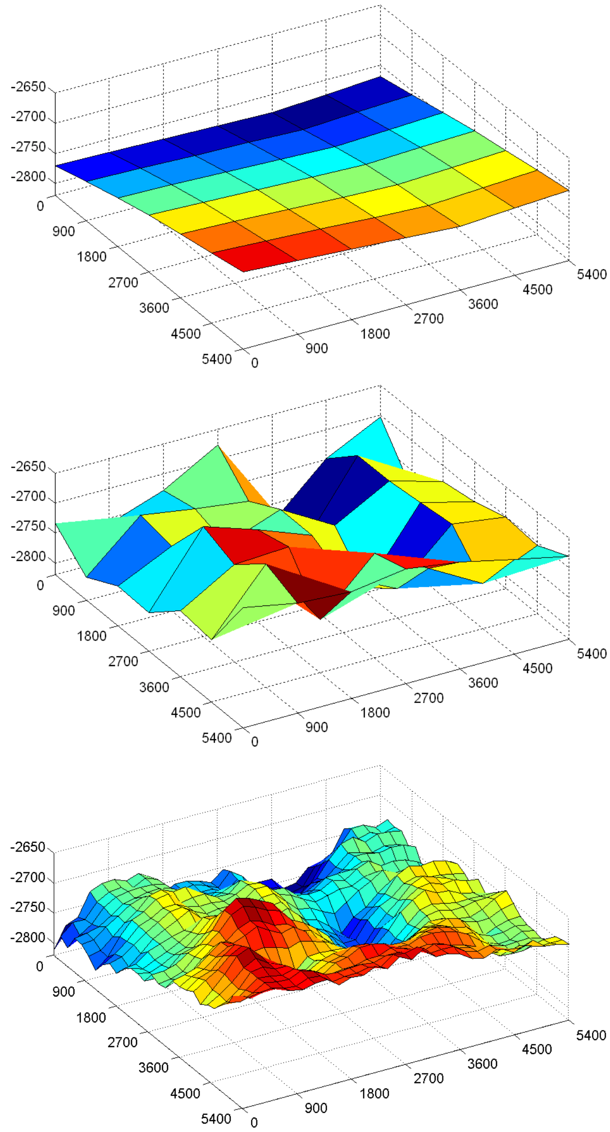

Fig. 4: Perspective views of the valley DTM in various processing steps; top: MOLA (sampling points densified to match the first facet size of 900 m), center: result of the first calculation step, bottom: final DTM.

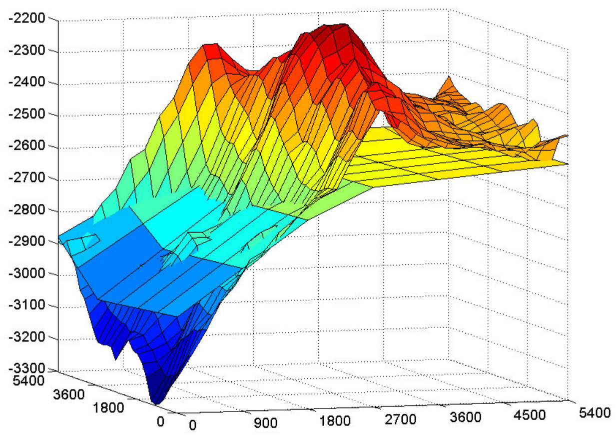

Fig. 5: Combined perspective view of the initial MOLA heights and the final DTM for the crater rim.

It.	900^2	450^2	300^2	200^2
Valley area:				
1	23.5 ± 3.9	20.8 ± 7.3	20.3 ± 10.8	26.7 ± 16.2
2	9.0 ± 3.6	7.1 ± 7.2	6.6 ± 10.7	8.3 ± 15.9
3	3.1 ± 3.6	2.5 ± 7.2	2.5 ± 10.6	4.0 ± 15.9
4	1.0 ± 3.6	1.2 ± 7.2	1.6 ± 10.7	2.8 ± 15.8
Crater rim:				
1	66.4 ± 6.4	43.3 ± 7.6	37.8 ± 9.8	34.1 ± 13.8
2	40.0 ± 4.5	34.8 ± 6.5	36.0 ± 9.3	31.9 ± 13.5
3	47.5 ± 4.2	34.7 ± 6.3	35.5 ± 9.3	31.4 ± 13.5
4	47.8 ± 4.2	33.6 ± 6.3	35.0 ± 9.2	31.1 ± 13.4

Table 2: Absolute height changes and standard deviations (median values) in [m] for both of the test areas.

By looking at Table 2, it can be seen that the average height changes (absolute values) in the valley region reduce towards zero over the iterations, while for the crater rim they don't. This is due to the low pass filtering, which causes larger absolute height changes in this steep terrain than in the flat valley. Without filtering, the height corrections would further decrease but, on the other hand, few outliers occur especially at the less constrained terrain borders and edges (cp. *Gehrke* et al., 2006) However, smaller facet sizes in subsequent calculation steps allow for the modelling of finer surface features, and new corrections in height arise. In both regions, these corrections are barely significant for the smallest facets. Due to the decrease of facet sizes the number of grey value observables per facet reduces noticeably and the standard deviations (RMS) increase with every calculation step. Although both regions feature different characteristics, the standard deviations are similar. Thus, the accuracy seems to depend predominantly on imaging conditions (resolution, etc.), which are identical in our case.

4. VALIDATION OF THE RESULTS

In order to compare both results obtained by *Facets Stereo Vision* the final object models are combined, i.e. the orthoimages are overlaid with contour lines derived from the DTMs. HRSC orbit 894, which these investigations are based on, has also been processed with the adaptive method by *Gwinner* et al. (2005). The DTM, featuring a resolution of 50 m, offers the possibility to independently compare our results. Contours are also derived from this model and laid on top of systematically processed nadir orthoimage portions (*Scholten* et al., 2005). The topographies are shown in Fig. 6 for the valley and in Fig. 7 for the crater rim. The good agreement between orthoimages and DTMs on one hand as well as between different algorithms on the other hand is evident. Apart from very flat terrain, contour lines run quite similar, although the result from adaptive processing appears smoother, which is due to the nominal resolution of 50 m. It should be pointed out, that our results are based on only 27x27 facets.

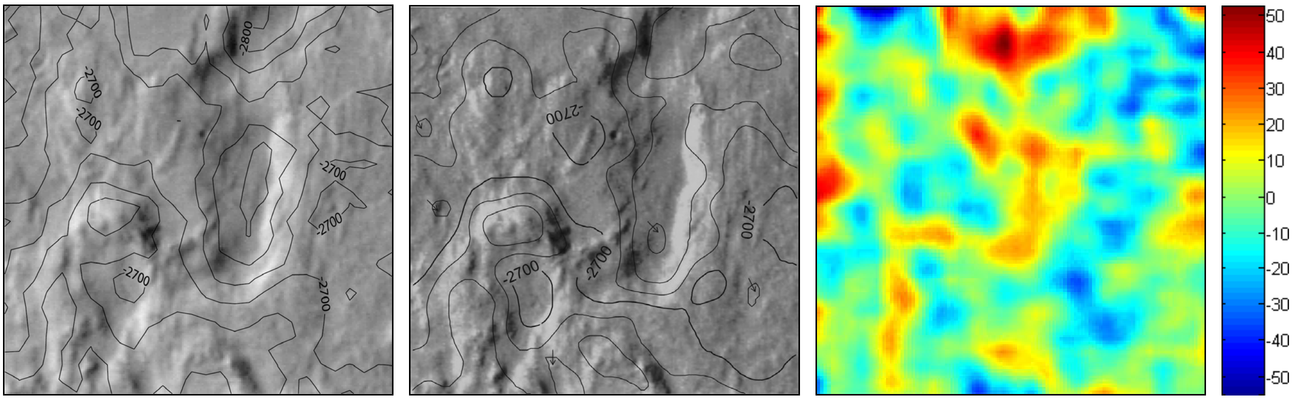

Fig. 6: Orthoimage and contour lines (equidistance of 25 m) based on the results of *Facets Stereo Vision* (left) and adaptive processing (center) as well as DTM height differences (right) for the valley region.

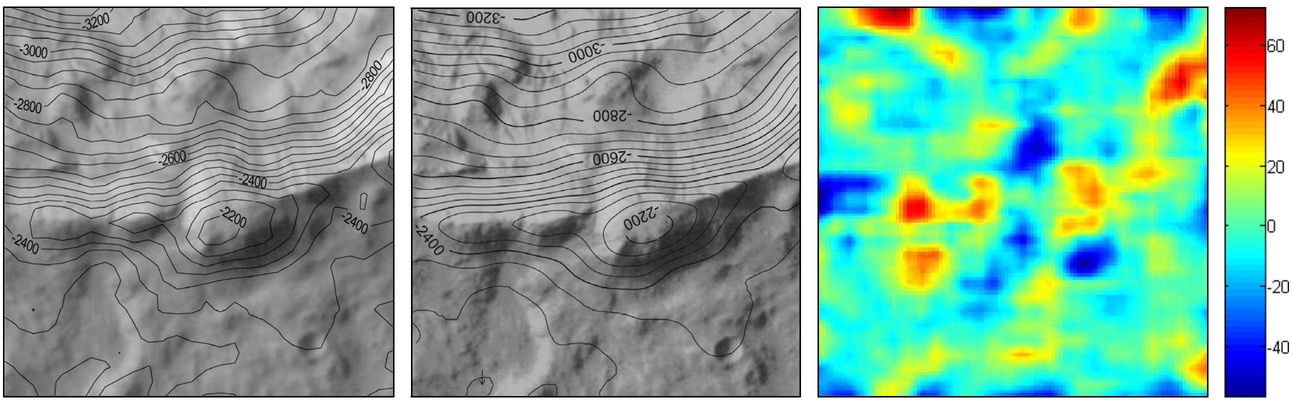

Fig. 6: Orthoimage and contour lines (equidistance of 50 m) based on the results of *Facets Stereo Vision* (left) and adaptive processing (center) as well as DTM height differences (right) for the crater rim.

A quantitative comparison can be achieved by subtracting both DTMs. The height differences are listed in Table 3; color-coded illustrations are given in Fig 5 and Fig 6. The very good agreement is confirmed by the height offsets (mean differences) between the respective models as well as the standard deviations, i.e. the RMS' of particular differences that nicely match with our accuracies of the final adjustments (cp. Table 2). As expected, the maximum deviations occur at the borders, which are less constrained in the *Facets Stereo Vision* algorithm.

	Valley area	Crater rim
Offset/mean difference	-1.3	0.1
Minimum difference	-55.7	-57.9
Minimum difference	53.3	73.2
RMS in [m]	14.1	16.7

Table 2: Comparison of *Facets Stereo Vision* and adaptive processing – differences in [m].

5. SUMMARY AND OUTLOOK

In this study, first experiences with the application of *Facets Stereo Vision* to HRSC on *Mars Express* line scanner imagery have been made. Using the MOLA 5 km DTM as initial values, meaningful results for the object properties – greyscale orthoimages and DTMs with ground resolutions of 25 m and 200 m, respectively – have been derived by successive decrease of DTM facet sizes. The results for two areas with different surface characteristics, a steep crater rim and a comparatively flat valley, are in very good agreement with independently derived products.

With the presented results as well as with the application on other regions of the Martian surface, the *Facets Stereo Vision* algorithm has to be further investigated, especially regarding initial heights and regularization aspects (*Wrobel* et al., 1992). Regularization may allow for calculations with smaller facets.

Facets Stereo Vision is flexible to the determination of further parameters, e.g. to represent the transfer function with a qualified surface reflectance model. In our calculations, linear functions have been applied to adjust contrast and brightness between the images. Such an approach is not physically motivated and does not model direction-dependant reflectance. Therefore, *Lambert's* reflectance law, which consists of a sole parameter, the overall surface albedo, is implicitly assumed. The inclusion of a sophisticated reflectance model will be subject to future work.

REFERENCES

Albertz, J., Attwenger, M., Barrett, J., et al., 2005b. HRSC on Mars Express – Photogrammetric and Cartographic Research. *Photogrammetric Engineering & Remote Sensing*, Vol. 71, No. 10, pp. 1153-1166.

Anderssohn, J., 2004. *Untersuchungen zur objektraumbasierten Bildrekonstruktion (Facetten-Stereosehen) an Hand von Bilddaten der Mars-Oberfläche*. Diploma Thesis, TU Berlin.

Diehl, H., Heipke, C., 1992. Surface Reconstruction from Data of Digital Line Cameras by Means of Object Based Image Matching. *International Archives of Photogrammetry and Remote Sensing*, Washington, Vol. XXIX, Part B3, pp. 287-294.

Gehrke, S., Schneider, I., Neukum, G., 2006: Combined Derivation of Orthoimages and DTM from Mars Express HRSC Data by Means of Matching in Object Space. – *Proceedings 5th Turkish-German Joint Geodetic Days*, Berlin.

Gwinner, K., Scholten, F., et al., 2005: Hochauflösende Digitale Geländemodelle der Marsoberfläche. *Photogrammetrie – Fernerkundung – Geoinformation (PFG)*, 5/2005, pp. 387-394.

Heipke, C., Oberst, J., et al., 2006: The HRSC DTM Test. *The International Archives of Photogrammetry and Remote Sensing*, Goa, Vol. XXXVI, Part B4 (this conference).

Neukum, G., et al., 2004. The High Resolution Stereo Camera of Mars Express. *ESA Special Publication SP-1240*.

Schlüter, M., 2000. Multi-Image Matching in Object Space Using Airborne CCD-Linescanner Imagery. *The International Archives of Photogrammetry and Remote Sensing*, Amsterdam, Vol. XXXIII, Part B3.

Scholten, F., Gwinner, K., Roatsch, T., et al., 2005. Mars Express HRSC Data Processing – Methods and Operational Aspects. *Photogrammetric Engineering and Remote Sensing*, Vol. 71 (10), pp. 1143-1152.

Smith, D.E. et al., 2001: *Mars Orbiter Laser Altimeter: Experiment Summary after the First Year of Global Mapping of Mars.* Journal of Geophysical Research, Vol. 106, E10, pp. 23,689-23,722.

Spiegel, M., Stilla, U., Giese, B., et al., 2005. Bündelausgleichung von HRSC-Bilddaten mit Mars Observer Laser Altimeter-Daten als Passinformationen. *Photogrammetrie – Fernerkundung – Geoinformation*, 5/2005, pp. 381-386.

Weisensee, M., 1992. *Modelle und Algorithmen für das Facetten-Stereosehen.* Dissertation, DGK-Reihe C, Vol. 374.

Wendt, A., 2002. Gemeinsame Ausgleichung von Laserscannerdaten und digitalen photogrammetrischen Bildern. *Photogrammetrie – Fernerkundung – Geoinformation*, Vol. 2/2002, pp. 103-110.

Wrobel, B.P., 1987. Facets Stereo Vision (FAST Vision) – A New Approach to Computer Stereo Vision and to Digital Photogrammetry. *Proceedings Intercommission Conference on Fast Processing of Photogrammetric Data*, Interlaken.

Wrobel, B.P., Kaiser, B., Hausladen, J., 1992. Adaptive Regularization – A New Method for Stabilization of Surface Reconstruction from Images. *The International Archives of Photogrammetry and Remote Sensing*, Washington, Vol. XXIX, Part B3, pp. 824-831.

ACKNOWLEDGEMENTS

The research project *Software Development and Technical Support for Cartographic Data Processing* at the *Technische Universität Berlin* is funded by the German *Bundesministerium für Bildung und Forschung.* This project is part of the research program *High Resolution Stereo Camera (HRSC) on the Mars Express Orbiter* under the guidance of Principal Investigator Prof. Gerhard Neukum, Freie Universität Berlin.

The authors thank Klaus Gwinner, DLR Berlin, for providing the high resolution DTM of HRSC orbit 894.